

Electrochemical study of amorphous $\text{Ni}_{89}\text{P}_{11}$ alloy in HCl solutions

SANAA TAHER ARAB

Department of Chemistry, Girls' College of Education, P.O (2321),
Jeddah 21451 (Kingdom of Saudi Arabia)

(Received: April 12, 2007; Accepted: June 04, 2007)

ABSTRACT

The electrochemical behavior of amorphous $\text{Ni}_{89}\text{P}_{11}$ alloy studied in HCl solutions at different concentrations in the range (1.0 – 9.0) shows that the alloy exhibit a passivation region at low concentrations and a pitting corrosion at higher concentration (9.0) M. This was explained to be due to the selective dissolution of Ni with consequent deposition of elemental phosphorus remaining on the alloy surface. The formation of the elemental phosphorous layer will acts as a diffusion barrier against nickel dissolution and the passivation is attended. With 9.0M HCl solutions an increase of Ni dissolution will occurred, pitting corrosion is found. X-ray photo-electron spectroscopy (XPS) is used to confirm these suggestions. The study of immersion time shows that the increase of the deposition of elemental phosphorus depending on the time of immersion. At the same time the dissolution of Ni continue, diffusion of the ions will occurred. A porous film is formed.

Key words: Metallic glasses, corrosion, electrochemical behavior, impedance, polarization, HCl solutions.

INTRODUCTION

Amorphous alloy have been found to possess various unique and attractive properties, including extremely high corrosion resistance. Even in hot concentrated hydrochloric acids, some of the amorphous alloys become spontaneously passive¹. They are in a thermodynamically metastable state, and hence they are chemically more reactive than the corresponding thermodynamic stable crystalline alloys. They can be regarded as a metallic solid with a frozen in melt structure²⁻⁴.

Amorphous Ni-P alloys are used to be known of significant commercial importance for corrosion protection, electronic device applications and catalysis^{5,6}. The corrosion behavior of these alloys has been studied extensively. They possess more excellent corrosion resistance than crystalline nickel metal,

and exhibit the peculiar anodic dissolution behavior. No apparent passive state appears in the anodic polarization curve, but the anodic current density is significantly low in acidic solutions^{7,8}.

The surface compositions of various amorphous Ni-P alloys after electrochemical treatment were determined and a large amount of phosphorous in various chemical states is enriched in the surface film⁷. Diegle *et. al.*⁹⁻¹¹ measured X-ray photo electron spectra from amorphous Ni-P alloy specimens. They proposed that the passivity was due to the adsorption of hypophosphite anion. Habazaki *et. al.*¹² suggested that an elemental phosphorous layer was formed on the surface of amorphous $\text{Ni}_{81}\text{P}_{19}$ alloy immersed in 1.0 M HCl solution at 30°C as a result of preferential dissolution of nickel, the low corrosion rate of amorphous Ni-P alloy in strong acids is attributed to the

formation of the elemental phosphorous layer which acts as a diffusion barrier against nickel dissolution. The formation of an elemental phosphorous layer acting a diffusion barrier against dissolution explains the almost constant corrosion rate regardless of HCl concentration¹³.

The electrochemical behavior of amorphous Ni-P alloys has not been clearly understood. The present work aims to study the effect of the concentration of HCl and the immersion time on the electrochemical behavior of Ni₈₉P₁₁ alloy.

EXPERIMENTAL

Ni₈₉P₁₁ alloy ingots supplied by Vacuumschmelze as ribbon (0.025 × 25.0mm), was used as working electrode. Electrochemical measurements were made on the bright face (24 mm²) without any mechanical polishing before each experiment. The dull face being masked by chemically inert resin which does not react with the chemical used as electrolyte. The electrode was degreased with alcohol and rinsed several times with bi-distilled water and finally cleaned in an ultrasonic bath. The used HCl was of reagent grade. Appropriate concentrations of aerated HCl were prepared by dilution using bi-distilled water.

Electrochemical measurements have been achieved by connecting the electrochemical cell to ACM Gill AC instrument and to personal computer. Polarization curves were measured form potentiodynamically cathodically then anodically with a potential sweep rate of 60 mV/min after open circuit immersion for 15 min. The reference electrode used in this study was a saturated calomel electrode (SCE). Impedance (EIS) data was obtained in the frequency range 10 KHz - 0.5Hz. The effect of immersion time on the corrosion processes of the studied alloy at certain concentration was carried out by electrochemical and morphological studies.

X-ray photo-electron spectroscopy (XPS) technique was used to give more information's about the composition on the surface before and after the corrosion reaction. From the binding energy of a

photoelectron peak, the elemental identity and chemical state of an element are determined. X-ray photo-electron spectra from the alloy surface were measured by a multi-technique surface analysis system (MAX200, Leybold) with MgK_α and AlK_α at 100W of x-ray power. For the analysis of corrosion products and surface films by means of XPS, data regarding spectra of standard substances are required¹⁴.

The scanning electron microscopy (SEM) is a microscope that uses electron rather than light to form an image. The combination of higher magnification larger depth of focus, greater resolution, and ease of sample observation makes the SEM one of the most heavily used instruments in research areas today.

In this study Scanning electron microscopy instrument of (XL20-PHILPS) was used. Sample was cut to specimen of 0.4 cm by 0.7cm and coated by conductive material (Gold).

Electrodes used for XPS and SEM were prepared as mentioned before and polarized to an anodic passive potential and then the electrodes were removed form the electrolyte and stored in a bottle under dried nitrogen N₂ (99.99%) until being transferred in to the apparatus for the surface analysis. The analysis took place immediately after transfer.

RESULTS AND DISCUSSION

Acid concentration effect

The potentiodynamic polarization curves of Ni₈₉P₁₁ in Fig. 1 with various concentrations (1.0,

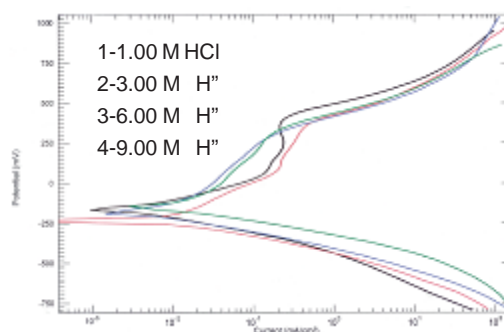


Fig.1: Potentiodynamic polarization curves of Ni₈₉P₁₁ glassy alloy at concentrations of HCl.

3.0, 6.0, and 9.0 M) of HCl gave almost the same behavior. It can be seen from the figure that nickel dissolution occurred at nearly -250 mV then a narrow unstapled passive region is observed. Gradual increase of the current density up to the current limit is then observed, indicating that the dissolution through the passive film is occurring. The width of the active to the passive transition at which the corrosion rate reaches its kinetic limit decrease with increasing the acid concentration. The obtained potential values are in the range of (100-350) mV, corresponding to small changes in current density. A likely explanation of the formed surface layer on the alloy specimens during potentiostatic polarization was suggested before to be consist of elemental phosphorus^{7,12,13}. It was statutes that the obtained results of X-ray photo-electron spectra measurements for specimens transferred to XPS apparatus under argon atmosphere after polarization in 3.0M HCl, confirmed that P⁺ ion were found in the surface region as well as elemental phosphorus, and the nickel ion was not found¹². In this study the same finding is obtained, the study

of XPS of the alloy in 3.0M HCl, Fig.(2) in which the relation between binding energy and intensity for Ni and P in the alloy as received and in HCl solution, shows that nickel does not cooperate to produce passive film. The obtained band for Ni^m 2p_{3/2} is 852.7 eV and no change is found, and dissolution of Ni is occurred. It is also, shows that the formation of elemental phosphorus is confirmed by the presence of a band at 130 eV¹⁴. These findings suggested that the anodic polarization of amorphous Ni-P alloy in acids in the potential region up to 400 mV leads to selective dissolution of nickel with a consequent formation of an elemental phosphorus layer on the alloy surface because the dissolution rate constant of nickel is larger than that of phosphorus¹³. Inspection of Figures (1&2) show that , the presence Cl⁻ ions which are know to be aggressive will facility the Ni dissolution, the formation of stable compact layer is not expected .The data given in Table (1) indicates that the values of I_{corr} increases with increasing [HCl] reveling increase in corrosion rate. But the appearance of small passive area is

Table 1: Electrochemical parameters for Ni₈₉P₁₁ alloy at different concentrations of HCl at 30°C

C _{HCl} (M)	Polarization					Impedance		Corrosion rate mm/y
	-E _{corr} mV/SCE	I _{corr} × 10 ² mA/cm ²	β _a mV/dec	β _c mV/dec	R _{ct} (Ωcm ²)	CPE(Q) (μF/cm ²)	n	
1.0	153	3.235	0.086	0.092	8065	41.85	0.77	0.82
3.0	222	3.748	0.084	0.085	6960	42.99	0.72	0.70
6.0	190	7.655	0.088	0.084	3392	75.65	0.86	0.31
9.0	170	21.96	0.093	0.081	1208	54.71	0.84	0.13

attributed to the deposition of elemental phosphor¹⁵. The formation of an adsorbed film of Cl⁻ on the alloy surface was detected by XPS, Fig. (2) a band at 198.7 – 197.8 eV , it was found to be corresponding to the presence of adsorbed Cl⁻¹⁴.

The electrochemical parameters of polarization in the studied acids are listed in Table (1). The table shows that the corrosion current I_{corr} and the corrosion potential E_{corr} decreased with the increase of acids concentration. While β_c and β_a are slightly effected.

The EIS measurements were carried out for the alloy at various concentrations of HCl after the alloy reached the steady - state potential after about 15 min. The electrochemical impedance spectroscopic technique helps to isolate the individual components describing the particular processes and properties of phases and interfaces, electrolyte resistance, charge transfer resistance (the fast process), doable layer capacitance, adsorption and diffusion (the lowest process)¹⁶.

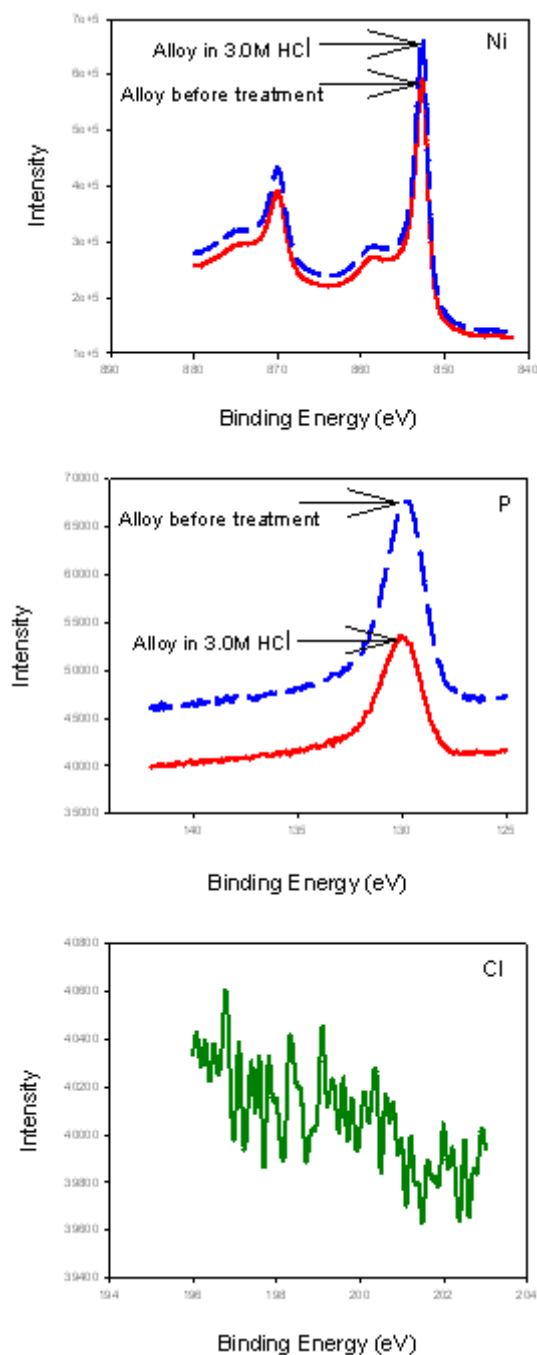


Fig. 2: The photo-electron spectra obtained for $\text{Ni}_{89}\text{P}_{11}$ glassy alloy before and after the experiment in 3.0M HCl .

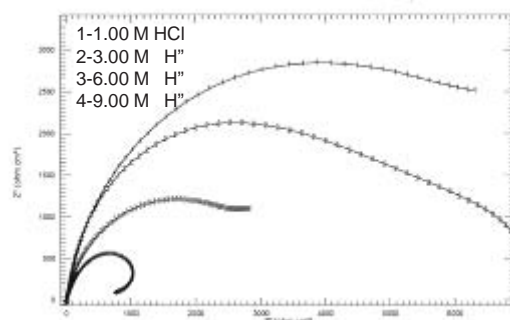


Fig. 3: Impedance plots of $\text{Ni}_{89}\text{P}_{11}$ glassy alloy in different concentrations of HCl.

EIS spectra, in Fig.(3), (Nyquist plot) exhibit only one capacitive semicircles with an open end in most of applied frequency range at low concentrations (1.0 and 3.0) M. The capacitive loop mainly due to the combination of the charge transfer resistance and the capacitance at the alloy / solution interface (dielectric properties of the surface), while the inductive loop at low frequencies indicating localized attack¹⁷. The diagrams sometimes show a capacitive arc at high and intermediate frequencies range followed by a tail at lower frequencies. The capacitive arc may be related with the dielectric properties of a formed film on the electrode surface and /or related to the electric double layer capacitance at the electrode / solution interface, which includes a metal / film interface followed by a film / solution interface¹⁸. he found tail in 6.0M, is probably associated with mass transport process in the solution.

Analysis of the impedance spectra is done by fitting the experimental data to equivalent circuit developed by Boukamp¹⁹. The quality of fitting to the equivalent circuit (EC) was judged firstly by the chi-square (χ^2) values and secondly by the error distribution versus frequency, comparing experimental with simulated data.

The Nyquist diagrams on HCl solutions were characterized by depressed capacitive loops with the theoretical centre located below the real axis at 1.0, 3.0 and 6.0 M. So, the measured capacitive response is not generally ideal (i.e.a pure capacitor). A constant phase element (CPE) is introduced for the spectra fitting, instead of

an ideal capacitance element. The impedance expression of CPE is given by^{8, 20}.

$$Z_{CPE} = \frac{1}{Q(j\omega)^n}$$

Where Q and n are frequency-independent fit parameters, j = (-1)^½ the imaginary number and $\omega=2\pi f$, the angular frequency in radius. The factor n, the CPE exponent, is an adjustable parameter. In general, it is believed that the CPE is related to some type of heterogeneity of the electrode surface as well as to the fractal nature (roughness or porosity) of the surface^{17,18,21}.

In 9.0 M of HCl solutions an inductive loop at low frequencies is found which indicated localized attack¹⁷. This may be explained as a result of increasing HCl concentration which will cause more and more of Ni dissolution leading to the breakdown of the barrier film which consists of elemental phosphorous, pitting corrosion will occur. This confirmed the idea that Cl⁻ migrate through the barrier film formed on alloy leading to the formation of Ni²⁺ ions, which leads to pitting of the alloy surface. Badawy *et al.*²² show that the adsorption of Cl⁻ on Cu-Ni alloys enhances the rate of diffusion of metal ions from metal film interface to the films / solution interface leading to the formation of cation vacancies, a pitting on the alloy surface is found. Moreover, complex halide possessing good solubility may also be formed pitting corrosion. Thus, it is possible to explain the general mechanism for pitting initiation that developed on the amorphous alloy by the Cl⁻ anions as follows: by virtue of its smaller size and larger polarizability, Cl⁻ anion become strongly adsorbed on the barrier film creating an electrostatic field and accumulating of Ni²⁺ in solution through the elemental phosphorous film. The magnitude of the field depends upon the thickness of this film as well as on the adsorbed negatively charged density. The negative charge density resulting from the adsorption of Cl⁻ anion can be expected to create an equal and opposite charges on the metal side of the film. When this ultimately reaches a critical density, a local breakdown

through the film takes place and Cl⁻ anions reached bare metal representing onset of pitting corrosion initiation. Similar observation was shown by El-Naggar¹⁷.

Corrosion kinetic parameters derived from EIS measurements are given in Table (1). The corrosion rate is widely accepted to be inversely proportional to the polarization resistance R_{ct}. The large R_{ct} value, the better corrosion resistance. R_{ct} is a measure of the corrosion rate, from the values of R_{ct} obtained in the investigated HCl solutions, it is observed that there is regular decrease (about 15 %) in R_{ct} values by increasing in aggressive [Cl⁻] from 1.0 to 9.0M.

The values of Q, associated to the CPE, increase with [Cl⁻] increase over the alloy surface. The values of n obtained (~0.80) indicates that the CPE is little associated with the film capacitance processes, certainly at high acid concentration due to pitting process²³. Table (1) also represent the values of corrosion rate at mm/y calculated by impedance measurements. It is clear that increasing the aggressive ion in the test solution increase the value of corrosion rate.

The colorless test solution turned to light green and the samples corroded completely at the interface at the highest [HCl], where the intensity of the color increase. The rapid dissolution of the alloy at interface in 9.0 M of acid is attributed to localized corrosion (crevice or pitting) as shown in Nyquist spectra.

Ismail *et al.* [24], revealed that the species such as Ni (H₂O)_{ads}, NiCl_{ads} and / or NiClOH_{ads} are adsorbed at the surface of NiCu alloys in chloride solutions. The desorption of the intermediate species produces new active sites on the electrode surface. So, the formation of the passive film is hindered leading to a localized metal dissolution.

Figure (4) shows ESM of the alloy surface after the electrochemical study in 3.0M of HCl solutions. It can be seen that no passive layer is



Fig. 4: Scanning electron micrographs of Ni₈₉P₁₁ glassy alloy at different magnifications in 3.0 M HCl solution.

detected, the surface is covered only by the residue which is composed of elemental phosphorous. Small cracks are observed at a higher magnification.

Effect of immersion time

As shown in Fig.(5,a), the prolonging the exposure time (1-12) h of NiP alloy in 3.0M of HCl solution resulting an increase on its dissolution reaction, the Ni continues to dissolve, this will lead to more deposition of phosphorous element. The accumulation of phosphorous leads to presence of a passive region in the range -100 to 800 mV, which is an indication for film formation on the alloy surface. This was also reported by Zhang *et. al.*¹³. In general, passivation in aggressive solutions occurs as a result of preferential dissolution of alloy constituents unnecessary for passive film formation as reported by Kawashima *et. al.*⁷.

On the other side the increase in I_{cor}

values represent the decreasing in the protection efficiency of the formed film in HCl media due to [Cl⁻] adsorption as show on from XPS data, pitting is proposed to occur. In Table (2) the obtained electrochemical parameters are recorded, where the corrosion current density I_{corr} , the corrosion potential E_{corr} , the critical current I_{cc} and critical potential E_{cp} . As can be seen that an increase in E_{pp} at the beginning from 1 to 3 hours then a decrease is found. At the same time a decrease in I_{cc} is found This will supported the passivation at the beginning of immersion in HCl solutions. The electro-chemical parameters are listed in Table 3.

The Nyquist plots Fig. 5,b exhibit only one capacitive semicircle with an open end in all of studied immersion times. Its radius decreased by increasing the exposure time of the alloy in test solution. This indicates that diffusion process is take-in place through the formed film; the penetration of

Table 2: Electrochemical parameters for Ni₈₉P₁₁ alloy at different immersion times in 3.0 M of HCl at 30°C.

Time (h)	Polarization									Impedance CPE(Q) n
	$-E_{corr}$ mV/SCE	$I_{corr} \times 10^2$ mA/cm ²	E_{pass} mV/SCE	E_{pp} mV/SCE	I_{cc} mA/cm ²	$E_{i_{pass}}$ mV/SCE	Rct (Ω cm ²)	C_{dl} (μ F/cm ²)	CPE(Q) (μ F/cm ²)	
1.0	212.97	4.12	232.28	365.47	0.2227	0.2227	6.339	1.207	1.3085	0.83
3.0	229.1	5.98	565.68	809.97	1.176	1.7321	4.364	1.561	1.6079	0.88
6.0	301.22	6.18	188.11	254.76	0.1939	0.1967	4.235	3.238	3.505	0.86
9.0	253.17	8.46	166.3	277.36	0.2657	0.2533	2.799	5.348	5.685	0.90

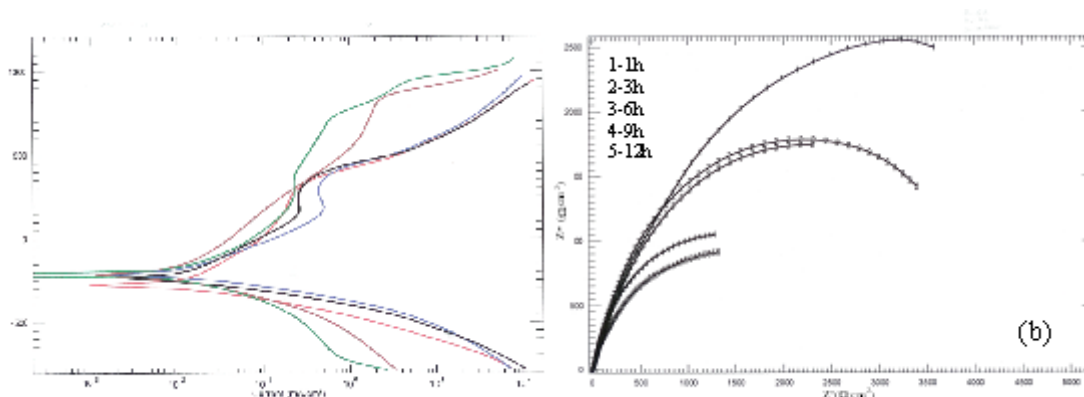


Fig. 5: Polarization (a) and Nyquist (b) curves of $\text{Ni}_{89}\text{P}_{11}$ metallic glass corrosion at different immersion times at 3.0 M HCl solutions

Ni^{+2} through elemental phosphorus, this will produce a less protecting properties, metal dissolution continues and an increase in dissolution current I_{corr} will be recognized. The obtained almost perfect semicircle at low immersion time indicated a small susceptibility to pitting corrosion and passivation is found. The capacitive loop is mainly due to the combination of the charge transfer resistance and the capacitance behavior at the alloy / solution interface; the semicircle will be a merges between the formed film and the charged transfer loop [25]. In table (2) the obtained electrochemical parameters in which n value increases gradually with the increase of immersion time (1 - 9) hours, then a decrease is found. This supported the formation of

passive film at first followed by its brake down at (12) hours.

Conclusion

The $\text{Ni}_{89}\text{P}_{11}$ alloy shows unexpected behavior in HCl solutions, it gives passivation at low concentrations (3.0 – 6.0)M and at low immersion times (1.0 – 6.0) hours. HCl acid is known as aggressive media and the presence of passivation is not common. At the same time the increasing of each, acid concentration or immersion time a porous film will be produced. The Nickel dissolution will proceed with higher rates penetrating the formed phosphorus layer.

REFERENCES

1. K.Hashimoto, K.kobayashi, K.Asami and T.Masumoto, Proc. 8th Int. cong Metallic corrosion, P.70. Dechema, Frankurt (1981).
2. M.Maka, K.Hashimoto and T.Masumoto, *J. Japan Inst. Metals*, **38**, 835 (1974).
3. K.Hashimoto, K.Osada, T.Masumoto and S.Shimodaira, *Corros. Sci.*, **16**, 71 (1974).
4. D.Huerta and K.E.Heusler, proc. 9th Int. Cong Metallic Corrosion, P.222, National Research council Canada, Ottawa (1984).
5. S.Yoshida, H.Yamashita, T.Funabiki and T.Yonezawa, *J.Chem. Soc. Faraday Trans.*, **80**, 1435 (1984).
6. M.Fernandez, J.Martinez-Duart and J.Albella, *Electrochim. Acta*, **31**, 55 (1986).
7. K.Kawashima, K.Asami and K.Hashimoto, *J. Non-Cryst. Solids*, **70**, 69 (1985).
8. P.Nagartar, P.Searson and R.Latanision, Proc. Symp. Corrosion, Electrochemistry and catalysis of Metallic Glasses (Eds R.B.Diegle and Hashimoto), P 118, the electrochemical Society, Pennington (1988).
9. R.Diegle, N. Sorensen and G.Neison, *J.electrochem. Soc.*, **133**, 1769 (1986).
10. R.Diegle, C.Clayton, Y.Lu and N.Sorensen, *J.electrochem. Soc.*, **134**, 138 (1987).

11. R.Dielgle, N.Serensen, C.Clayton, M.Helfand and Y.Lu, *J.electrochem. Soc.*, **135**, 1085 (1988).
12. H.Habazaki, S.Dinf, A.Kawashima, K.Asami, K.Hashimoto, A.Inoue and T.Matsumoto, *Corros. Sci.*, **29**, 1319 (1989).
13. Bo.P.Zhang, H.Habazaki, A.Kawashima, K.Asmi and K.Hashimoto, *Corros. Sci.*, **33**, 667 (1992).
14. J. Chastain, "Handbook of X-ray Photoelectron Perkin - Elmer Corporation Spectroscopy", (1995).
15. 15.J.M. Le Canut, S. Maximovitch and F. Dalard, *J. Nucl. Mater.*, **334**, 13 (2004) .
16. 16M.M.Hukovic and S.Omanvic, *J. Electroanal. Chem.*, **455**, 181 (1998).
17. M. M.Naggar, *Appl. Surf. Sci.*, **252**, 6179 (2006).
18. P.Girault, J.L.Grosseau -Poussard, J.F.Dinhut and L .Marechal, *Nucl. Instrum. Methods Phys. Res., Sect. B*, **174**, 439 (2001).
19. B. A. Boukamp, *Equivalent Circuits (UserManual)*, University of Twente, the Netherlands, (1989).
20. E.M.A.Martini, S.T.Amaral and I.L.Muller, *Corros. Sci.*, **46**, 2097 (2004).
21. F.J.Perez, L.Martinez, M.P.Hierro, C. Gomez, A.L.Portela, G.N.Pucci, D.Duday, J. Lecomle - Beckers and Y. Greday, *Corros. Sci.*, **48**, 472 (2006).
22. W.A.Badawy, K.M.Ismail and A.M.Fathi, *Electrochim. Acta*, **50**, 3603 (2005).
23. G.W.Walter, *Corros. Sci.*, **32**,1041 (1991).
24. K.M.Ismail, A.M.Fathi and W.A.Badawy *Corros. Sci.*, **48**(8),1912 (2006).
25. Y.Chen, T.Hong, M. Gopal and W.P.Jepson, *Corros.Sci.*,**42**, 979 (2000).